SUPPLEMENTARY MATERIALS: NEURONAL RESILIENCE AND CALCIUM SIGNALING PATHWAYS IN THE CONTEXT OF SYNAPSE LOSS AND CALCIUM LEAKS: A COMPUTATIONAL MODELLING STUDY AND IMPLICATIONS FOR ALZHEIMER'S DISEASE*

PIYUSH BOROLE†, JAMES M. ROSADO‡, MEIROSE NEAL‡, AND GILLIAN QUEISSER‡

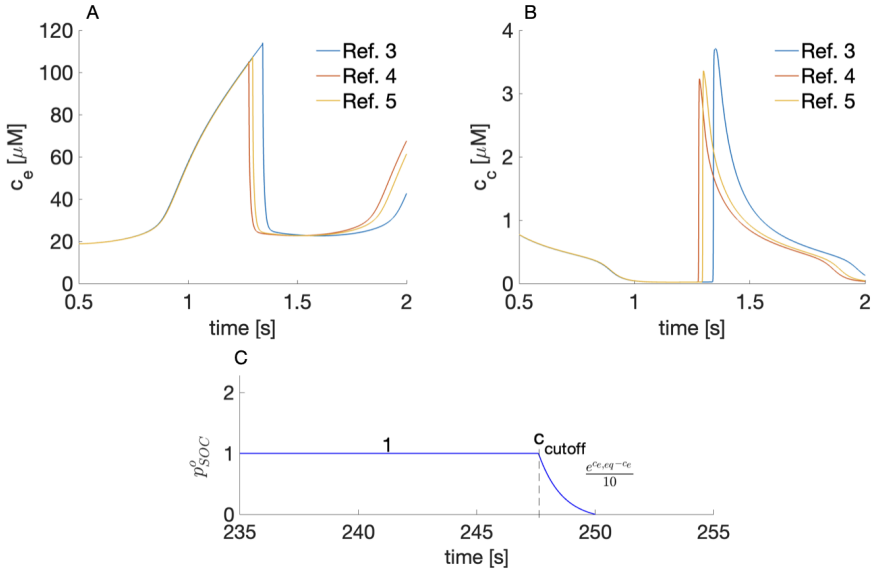

FIG. SM1. *Convergence analysis using different refinement levels. (A-B) concentration profiles for Ca^{2+} in the cytosol and ER, respectively on an unbranched neurite. The refinement levels were $m = 1, 2, 3, 4, 5$, with the edge length of $\Delta x = 2.0, 1.0, 0.5, 0.25, 0.125$ μm and time step $\Delta t = 160, 80, 40, 20, 10$ ms, respectively. (C) open state probability of SOC (p^o_{SOC}) is modeled after eq.* **??**. *The value of p^o_{SOC} is set to* 1 *until it reaches a cutoff value (*247.602 μM*, calculated) after which it decays exponentially to zero.*

*Submitted to the editors August 12, 2025
†University of Edinburgh, Edinburgh, Scotland, United Kingdom
‡Department of Mathematics, Temple University, Philadelphia, Pennsylvania, U.S.A.

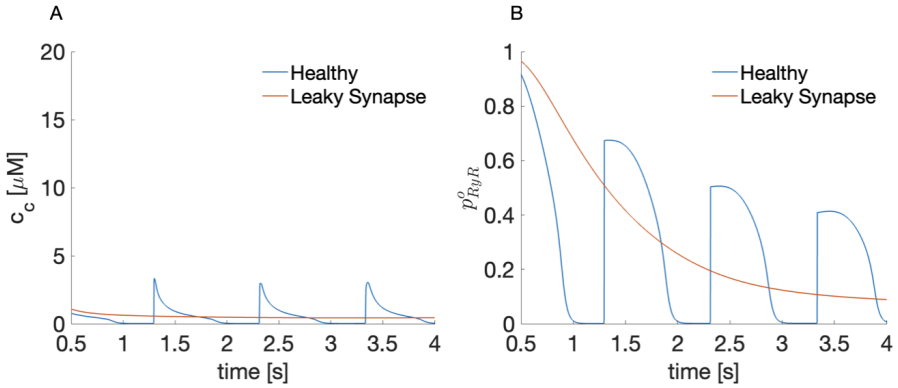

FIG. SM2. *RyR open state probability in healthy vs. leaky synapse in an unbranched neurite with 5Hz stimulation. (A) The Ca^{2+} profile at the soma in the healthy state causes 1Hz wave responses, where c_c is low during equilibrium. In leaky synapses, baseline c_c is elevated and no such wave response is observed. (B) The decrease of c_c levels to baseline in the healthy state allows p^o_{RyR} to also return to 0 after a wave event. However, in case of leaky synapses, the elevated c_c levels prevent p^o_{RyR} to return to 0 rapidly and thus hinders wave initiation.*

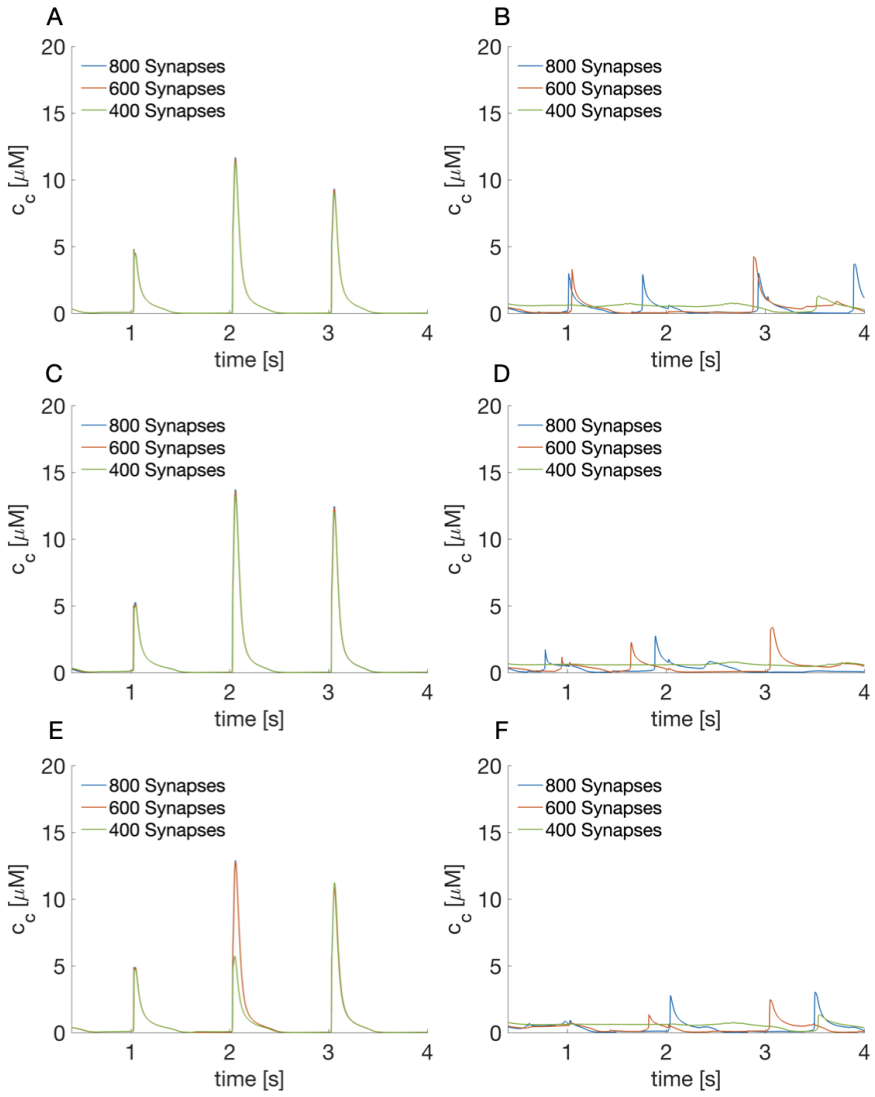

FIG. SM3. *Comparing different electro-calcium coupling. (A-B) no VDCCs, i.e., no eletrical coupling at 1Hz (A) and 5Hz (B) stimulation frequency. (C-D) N-Type VDCC coupling at 1Hz and 5Hz. (E-F) T-Type VDCC coupling at 1Hz and 5Hz. This figure is intended to illustrate that coupling the calcium dynamics to the electrical signal is relevant and different results are to be expected when excluding electro-calcium coupling or including different types of VDCC.*

TABLE SM1
Model Parameters

Parameter	Symbol	Value	Reference
		Initial and equilibrium values	
Cytosolic Ca^{2+}	c_c	50 nM	[SM4]
ER Ca^{2+}	c_e	250 μM	[SM4]
Reference ER Ca^{2+}	c_e^{ref}	250 μM	[SM4]
Extracellular Ca^{2+}	c_o	1 mM	[SM4]
Total Calbindin D_{28k} (Cytosol)	b^{tot}	40 μM	[SM19, SM4]
Total Calreticulin (ER)	b_e^{tot}	3.6 mM	[SM18]
		Diffusion/reaction	
Diffusion coefficient (c_c)	D_c	220 $\mu m^2 s^{-1}$	[SM1, SM4]
Diffusion coefficient (CalB)	D_c	20 $\mu m^2 s^{-1}$	[SM24, SM4]
CalB forward rate	κ_b^+	27 $\mu M^{-1} s^{-1}$	[SM19, SM4]
CalB backward rate	κ_b^-	19 s^{-1}	[SM19, SM4]
Diffusion coefficient (c_e)	D_{ce}	10 $\mu m^2 s^{-1}$	[SM6, SM17]
Diffusion coefficient (CalR)	D_{be}	27 $\mu m^2 s^{-1}$	[SM18]
CalR forward rate	κ_{be}^+	10^5 $M^{-1} s^{-1}$	[SM18]
CalR backward rate	κ_{be}^-	200 s^{-1}	Calculated using $K_d = 2$ mM ([SM2])
		RyR channel	
$o_1 \to c_1$	k_a^-	28.8 s^{-1}	[SM14]
$c_1 \to o_1$	k_a^+	1500 $\mu M^{-4} s^{-1}$	[SM14]
$o_2 \to o_1$	k_b^-	385.9 s^{-1}	[SM14]
$o_1 \to o_2$	k_b^+	1500 $\mu M^{-3} s^{-1}$	[SM14]
$c_2 \to o_1$	k_c^-	0.1 s^{-1}	[SM14]
$o_1 \to c_2$	k_c^+	1.75 s^{-1}	[SM14]
Reference current	I_{RyR}^{ref}	3.5×10^{-18} $mol\ s^{-1}$	[SM26]
		SERCA pumps	
SERCA current	I_S	6.5×10^{-21} $mol\ \mu M\ s^{-1}$	[SM5, SM4](Adapt.)
	K_S	180 nM	[SM25]
SERCA density	ρ_S	2390 μm^{-2}	[SM18](Approx.)
		PMCA pumps	
PMCA current	I_P	1.7×10^{-23} $mol\ s^{-1}$	[SM10]
Measure of Ca^{2+} affinity	K_P	60 nM	[SM8]
PMCA density	ρ_P	500 μm^{-2}	[SM4](Estim.)
		NCX pumps	
NCX current	I_N	2.5×10^{-21} $mol\ s^{-1}$	[SM10](adapt.)
Measure of Ca^{2+} affinity	K_N	1.8 μM	[SM10]
NCX density	ρ_N	15 μm^{-2}	[SM4](Estim.)
		Store Operated Channels	
Single SOC current	I_{SOC}^{ref}	2.1 fA	[SM9, SM13]
Faraday's Constant	F	96485 C/mol	
Valency of Ca^{2+} ion	z	2	
Density of SOC	ρ_{SOC}	0.4 μm^{-2}	choosen
		Aβ pores	
Rate constant	k_β	1 s^{-1}	[SM16, SM7]
Cooperative factor	m	4	[SM16, SM7]
Concentration of Aβ	a	5 nM, 100 μM	[SM7, SM20]
		Miscellaneous	
Input synaptic flux	j_{syn}	1×10^{-6}	[SM4, SM23]

TABLE SM2
Model Parameters for VDCCs and electrical dynamics equations

Parameter	Symbol	Value	Reference
	Voltage Dependent Calcium Channels (VDCC) N-type		
Valence	z_k, z_l	2, 1	[SM11, SM3]
Voltage	$V_{1/2,k}, V_{1/2,l}$	-21 mV, -40 mV	[SM11, SM3]
Rate parameter	γ_k, γ_l	0, 0	[SM11, SM3]
Rate parameter	K_k, K_l	1.7 ms, 70 ms	[SM11, SM3]
Time constant	$\tau_{0,k}, \tau_{0,l}$	1.7 ms, 70 ms	[SM11, SM3]
Permeability of Ca^{2+}	$\bar{p}_{\mathrm{Ca}^2+}$	3.8 cm^3/s	[SM11, SM3]
Faraday Constant	F	96485 C/mol	[SM11, SM3]
Gas Constant	R	8.314 J/Kmol	[SM11, SM3]
Temperature	T	310 Kelvin	[SM11, SM3]
	Voltage Dependent Calcium Channels (VDCC) T-type		
Valence	z_k, z_l	2,1	[SM3]
Voltage	$V_{1/2,k}, V_{1/2,l}$	-36 mV, -68 mV	[SM3]
Rate parameter	γ_k, γ_l	0,0	[SM3]
Rate parameter	K_k, K_l	1.5 ms ,10 ms	[SM3]
Time constant	$\tau_{0,k}, \tau_{0,l}$	1.5 ms, 10 ms	[SM3]
Permeability of Ca^{2+}	$\bar{p}_{\mathrm{Ca}^2+}$	1.9 cm^3/s	[SM11, SM3]
	Parameters for Electrical Dynamics		
Axonal Resistance	R_{ax}	0.75 $\Omega \cdot m$	[SM21]
Membrane Capacitance	C	0.01 F/m^2	[SM21]
K^+ Conductance	$\bar{g}_K$	50 S/m^2	[SM21]
Na^{2+} Conductance	$\bar{g}_{Na}$	500 S/m^2	[SM21]
Leak Conductance	$\bar{g}_l$	0.05 S/m^2	[SM21]
K^+ Reversal Potential	V_K	-0.90 V	[SM21]
Na^{2+} Reversal Potential	V_{Na}	0.50 V	[SM21]
Leak Reversal Potential	V_l	-0.60 V	[SM21]
Ca^{2+} Reversal Potential	V_{Ca}	A function of Ca^{2+}	[SM22, SM15]
Initial K^+ Channel Probability	n_0	0.00654	[SM12]
Initial Na^{2+} Channel Probability	m_0	0.00654	[SM12]
Initial Na^{2+} Channel Probability	h_0	0.9997	[SM12]
Initial Ca^{2+} Channel Probability	σ_0	0.9750	[SM22, SM15]
Calcium Current Parameter	K	0.01 mol/m^3	[SM22, SM15]

SM1. Derivation for 1D reduced model. In this section, we derive the 1D reduced PDEs for cytosolic Ca^{2+} concentration c_c. Fig. SM4 illustrates a section of unbranched neurite of width dx. The ER radius and the dendrite radius are denoted by r and R respectively. The fluxes (J_{PM}) between cytosolic (Ω_C) and extracellular domain are on boundary Γ_{PM} while the fluxes (J_{ERM}) between ER (Ω_{ER}) and cytosolic doamins are on boundary Γ_{ERM}. At a given point, surface area of $\Gamma_{PM} = 2\pi R$ and $\Gamma_{ERM} = 2\pi r$. The area of $\Omega_C = \pi(R^2 - r^2)$ and $\Omega_{ER} = \pi r^2$.

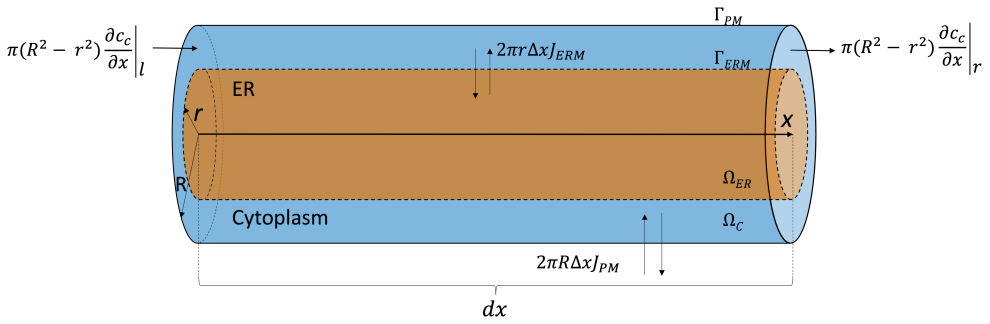

FIG. SM4. *Illustration of a section of an unbranched neurite of width dx displaying mechanisms affecting cytosolic Ca^{2+} concentration.*

We begin with the flux balance equation where each flux is scaled by the corresponding area/volume:

$$\begin{aligned}
\pi(R^2 - r^2)\Delta x\frac{\partial c_c}{\partial t} &= \left(\pi(R^2 - r^2)\frac{\partial c_c}{\partial x}\Big|_r - \pi(R^2 - r^2)\frac{\partial c_c}{\partial x}\Big|_l\right) + 2\pi r\Delta x J_{ERM} \\
&\quad +2\pi R\Delta x J_{PM} + \pi(R^2 - r^2)(k_b^-(b^{tot} - b) - k_b^+ b c_c) \\
(R^2 - r^2)\frac{\partial c_c}{\partial t} &= \frac{\left((R^2 - r^2)\frac{\partial c_c}{\partial x}\big|_r - (R^2 - r^2)\frac{\partial c_c}{\partial x}\big|_l\right)}{\Delta x} \\
&\quad +(R^2 - r^2)(k_b^-(b^{tot} - b) - k_b^+ b c_c) + 2r J_{ERM} + 2R J_{PM}
\end{aligned}$$

Dividing by Δx and taking Δx to 0 leads to:

$$\begin{aligned}
(R^2 - r^2)\frac{\partial c_c}{\partial t} &= \frac{\partial}{\partial x}\left((R^2 - r^2)\frac{\partial c_c}{\partial x}\right) + (R^2 - r^2)(k_b^-(b^{tot} - b) - k_b^+ b c_c) \\
&\quad +2r J_{ERM} + 2R J_{PM} \\
\frac{\partial c_c}{\partial t} &= \frac{1}{(R^2 - r^2)}\frac{\partial}{\partial x}\left((R^2 - r^2)\frac{\partial c_c}{\partial x}\right) + (k_b^-(b^{tot} - b) - k_b^+ b c_c) \\
&\quad +\frac{2r}{R^2 - r^2}J_{ERM} + \frac{2R}{R^2 - r^2}J_{PM}, \qquad \text{in } \Omega_C
\end{aligned}$$

Equivalently, we derive the 1D reduced equations for c_e, b and b_e:

$$\begin{aligned}
\frac{\partial c_e}{\partial t} &= \frac{1}{r^2}\frac{\partial}{\partial x}\left(r^2 D_c \frac{\partial c_e}{\partial x}\right) + \left(k_{be}^{-}(b_e^{tot} - b_e) - k_{be}^{+} b_e c_e\right) \\
&\quad -\frac{2}{r} J_{ERM} + \frac{2}{r} J_{SOC}, \qquad \text{in } \Omega_{ER} \\
\frac{\partial b}{\partial t} &= \frac{1}{(R^2 - r^2)}\frac{\partial}{\partial x}\left((R^2 - r^2) D_b \frac{\partial b}{\partial x}\right) + \left(k_b^{-}(b^{tot} - b) - k_b^{+} b c_c\right), \qquad \text{in } \Omega_C \\
\frac{\partial b_e}{\partial t} &= \frac{1}{r^2}\frac{\partial}{\partial x}\left(r^2 D_{be} \frac{\partial b_e}{\partial x}\right) + \left(k_{be}^{-}(b_e^{tot} - b_e) - k_{be}^{+} b_e c_e\right) \qquad \text{in } \Omega_{ER}
\end{aligned}$$

REFERENCES

[SM1] N. L. Allbritton, T. Meyer, and L. Stryer, *Range of messenger action of calcium ion and inositol 1, 4, 5-trisphosphate*, Science, 258 (1992), pp. 1812–1815.

[SM2] S. Baksh and M. Michalak, *Expression of calreticulin in escherichia coli and identification of its ca2+ binding domains.*, Journal of Biological Chemistry, 266 (1991), pp. 21458–21465.

[SM3] L. J. Borg-Graham, *Interpretations of Data and Mechanisms for Hippocampal Pyramidal Cell Models*, Springer US, Boston, MA, 1999, pp. 19–138, https://doi.org/10.1007/978-1-4615-4903-1_2, https://doi.org/10.1007/978-1-4615-4903-1_2.

[SM4] M. Breit and G. Queisser, *What is required for neuronal calcium waves? a numerical parameter study*, The Journal of Mathematical Neuroscience, 8 (2018), https://doi.org/10.1186/s13408-018-0064-x, https://doi.org/10.1186/s13408-018-0064-x.

[SM5] V. C. Chiu and D. H. Haynes, *Rapid kinetic studies of active ca2+ transport in sarcoplasmic reticulum*, The Journal of membrane biology, 56 (1980), pp. 219–239.

[SM6] M. J. Dayel, E. F. Hom, and A. S. Verkman, *Diffusion of green fluorescent protein in the aqueous-phase lumen of endoplasmic reticulum*, Biophysical journal, 76 (1999), pp. 2843–2851.

[SM7] J. De Caluwé and G. Dupont, *The progression towards alzheimer's disease described as a bistable switch arising from the positive loop between amyloids and ca2+*, Journal of theoretical biology, 331 (2013), pp. 12–18.

[SM8] N. L. Elwess, A. G. Filoteo, A. Enyedi, and J. T. Penniston, *Plasma membrane ca2+ pump isoforms 2a and 2b are unusually responsive to calmodulin and ca2+*, Journal of Biological Chemistry, 272 (1997), pp. 17981–17986.

[SM9] D. Gil, A. H. Guse, and G. Dupont, *Three-dimensional model of sub-plasmalemmal ca2+ microdomains evoked by the interplay between orai1 and insp3 receptors*, Frontiers in immunology, 12 (2021).

[SM10] M. Graupner, *A theory of plasma membrane calcium pump function and its consequences for presynaptic calcium dynamics*, Dissertation and Theses, (2003).

[SM11] S. Grein, M. Stepniewski, S. Reiter, M. M. Knodel, and G. Queisser, *1d-3d hybrid modeling-from multi-compartment models to full resolution models in space and time*, Frontiers in Neuroinformatics, 8 (2014), https://doi.org/10.3389/fninf.2014.00068, https://doi.org/10.3389/fninf.2014.00068.

[SM12] A. L. Hodgkin and A. F. Huxley, *A quantitative description of membrane current and its application to conduction and excitation in nerve*, The Journal of Physiology, 117 (1952), pp. 500–544, https://doi.org/10.1113/jphysiol.1952.sp004764, https://doi.org/10.1113/jphysiol.1952.sp004764.

[SM13] M. Hoth and R. Penner, *Depletion of intracellular calcium stores activates a calcium current in mast cells*, Nature, 355 (1992), pp. 353–356.

[SM14] J. Keizer and L. Levine, *Ryanodine receptor adaptation and ca2+ induced ca2+ release-dependent ca2+ oscillations*, Biophysical Journal, 71 (1996), pp. 3477–3487, https://doi.org/10.1016/s0006-3495(96)79543-7, https://doi.org/10.1016/s0006-3495(96)79543-7.

[SM15] C. Koch and I. Segev, *Methods in Neuronal Modeling: From Synapses to Networks*, A Bradford book, MIT Press, 1989, https://books.google.com/books?id=INvlQwAACAAJ.

[SM16] J. Latulippe, D. Lotito, and D. Murby, *A mathematical model for the effects of amyloid beta on intracellular calcium*, PloS one, 13 (2018), p. e0202503.

[SM17] E. McIvor, S. Coombes, and R. Thul, *Three-dimensional spatio-temporal modelling of store operated ca2+ entry: Insights into er refilling and the spatial signature of ca2+ signals*, Cell calcium, 73 (2018), pp. 11–24.

[SM18] S. Means, A. J. Smith, J. Shepherd, J. Shadid, J. Fowler, R. J. Wojcikiewicz, T. Mazel, G. D. Smith, and B. S. Wilson, *Reaction diffusion modeling of calcium dynamics with realistic er geometry*, Biophysical journal, 91 (2006), pp. 537–557.

[SM19] A. Müller, M. Kukley, P. Stausberg, H. Beck, W. Müller, and D. Dietrich, *Endogenous ca2+ buffer concentration and ca2+ microdomains in hippocampal neurons*, Journal of Neuroscience, 25 (2005), pp. 558–565.

[SM20] A. C. Paula-Lima, T. Adasme, C. SanMartin, A. Sebollela, C. Hetz, M. A. Carrasco, S. T. Ferreira, and C. Hidalgo, *Amyloid β-peptide oligomers stimulate ryr-mediated ca2+ release inducing mitochondrial fragmentation in hippocampal neurons and prevent ryr-mediated dendritic spine remodeling produced by bdnf*, Antioxidants & redox signaling, 14 (2011), pp. 1209–1223.

[SM21] M. Pospischil, M. Toledo-Rodriguez, C. Monier, Z. Piwkowska, T. Bal, Y. Frégnac, H. Markram, and A. Destexhe, *Minimal hodgkin–huxley type models for different classes of cortical and thalamic neurons*, Biological Cybernetics, 99 (2008), pp. 427–441, https://doi.org/10.1007/s00422-008-0263-8, https://doi.org/10.1007/s00422-008-0263-8.

[SM22] A. Protopapas, M. Vanier, and J. Bower, *Simulating large networks of neurons*, in Methods in Neuronal Modeling: From Synapses to Networks, MIT Press, 01 1998, pp. 461–498.

[SM23] J. M. Rosado, *Ultrastructural neuronal modeling of calcium dynamics under transcranial magnetic stimulation*, 2022, https://doi.org/10.34944/DSPACE/8010, https://scholarshare.temple.edu/handle/20.500.12613/8038.

[SM24] H. Schmidt, K. M. Stiefel, P. Racay, B. Schwaller, and J. Eilers, *Mutational analysis of dendritic ca2+ kinetics in rodent purkinje cells: role of parvalbumin and calbindin d28k*, The Journal of physiology, 551 (2003), pp. 13–32.

[SM25] J. Sneyd, K. Tsaneva-Atanasova, J. Bruce, S. Straub, D. Giovannucci, and D. Yule, *A model of calcium waves in pancreatic and parotid acinar cells*, Biophysical Journal, 85 (2003), pp. 1392–1405, https://doi.org/10.1016/s0006-3495(03)74572-x, https://doi.org/10.1016/s0006-3495(03)74572-x.

[SM26] A. Tinker, A. R. G. Lindsay, and A. J. Williams, *Cation conduction in the calcium release channel of the cardiac sarcoplasmic reticulum under physiological and pathophysiological conditions*, Cardiovascular Research, 27 (1993), pp. 1820–1825, https://doi.org/10.1093/cvr/27.10.1820, https://doi.org/10.1093/cvr/27.10.1820.